UNIVERSITY OF BIRMINGHAM
University of Birmingham Research at Birmingham

Throughput optimization in backscatter-assisted wireless-powered underground sensor networks for smart agriculture

Lin, Kaiqiang; Lopez, Onel Luis Alcaraz; Alves, Hirley; Chapman, David; Metje, Nicole; Zhao, Guozheng; Hao, Tong

DOI:
https://doi.org/10.1016/j.iot.2022.100637

License:
Creative Commons: Attribution-NonCommercial-NoDerivs (CC BY-NC-ND)

Document Version
Peer reviewed version

Citation for published version (Harvard):
Lin, K, Lopez, OLA, Alves, H, Chapman, D, Metje, N, Zhao, G & Hao, T 2022, 'Throughput optimization in backscatter-assisted wireless-powered underground sensor networks for smart agriculture', *Internet of Things*, vol. 20, 100637. https://doi.org/10.1016/j.iot.2022.100637

Link to publication on Research at Birmingham portal

Publisher Rights Statement:
This is the Accepted Author Manuscript of an article in Internet of Things published by Elsevier and available at https://doi.org/10.1016/j.iot.2022.100637

General rights
Unless a licence is specified above, all rights (including copyright and moral rights) in this document are retained by the authors and/or the copyright holders. The express permission of the copyright holder must be obtained for any use of this material other than for purposes permitted by law.

•Users may freely distribute the URL that is used to identify this publication.
•Users may download and/or print one copy of the publication from the University of Birmingham research portal for the purpose of private study or non-commercial research.
•User may use extracts from the document in line with the concept of 'fair dealing' under the Copyright, Designs and Patents Act 1988 (?)
•Users may not further distribute the material nor use it for the purposes of commercial gain.

Where a licence is displayed above, please note the terms and conditions of the licence govern your use of this document.

When citing, please reference the published version.

Take down policy
While the University of Birmingham exercises care and attention in making items available there are rare occasions when an item has been uploaded in error or has been deemed to be commercially or otherwise sensitive.

If you believe that this is the case for this document, please contact UBIRA@lists.bham.ac.uk providing details and we will remove access to the work immediately and investigate.

Download date: 27. Apr. 2024

Throughput Optimization in Backscatter-Assisted Wireless-Powered Underground Sensor Networks for Smart Agriculture

ARTICLE INFO

Keywords:
Sustainable smart agriculture
Backscatter communication
Wireless-powered underground sensor networks
Non-linear energy harvesting
Quality of service
Network throughput maximization

ABSTRACT

Wireless underground sensor networks (WUSNs) using wirelessly-connected buried sensors enable smart agriculture through real-time soil sensing, timely decision-making, and precise remote operation. Energy harvesting technology is adopted in WUSNs, implying wireless-powered underground sensor networks (WPUSNs), to prolong the network lifetime. In addition, the backscatter communication (BSC) technology seems promising for improving the utilization of resources and network throughput according to preliminary studies in terrestrial wireless-powered communication networks. However, this technique has not yet been investigated in WPUSNs, where channel impairments are incredibly severe. In this work, we aim to assess BSC's performance in WPUSNs and evaluate its feasibility for sustainable smart agriculture. For this, we first conceptualize a multi-user backscatter-assisted WPUSN (BS-WPUSN), where a set of energy-constrained underground sensors (USs) backscatter and/or harvest the radio frequency energy emitted by an above-ground power source before the sensed data are transmitted to a nearby above-ground access point. Then, we formulate the optimal time allocation to maximize the network throughput while assuring real-world users' quality of service (QoS). Our analysis considers the non-linearities of practical energy harvesting circuits and severe signal attenuation in underground channels. By simulating a realistic farming scenario, we show that our proposed solution outperforms two baseline schemes, i.e., underground harvest-then-transmit and underground BSC, by an average of 12% and 358% increase in network throughput (when USs are buried at 0.35 m), respectively. Additionally, several trade-offs between the network throughput, time allocation, network configurations, and underground parameters are identified to facilitate the practical implementation of BS-WPUSNs.

1. Introduction

Wireless underground sensor networks (WUSNs) consist of wirelessly-connected underground sensors (USs) deployed, for instance, for smart agriculture [1], underground infrastructure monitoring [2] , environmental monitoring [3], and disaster rescue [4]. Especially, tackling the doubling of food demand by 2050, smart agriculture is adopting WUSN technology based on accurate *in-situ* information, timely decision-making, and precise remote operation to obtain more efficient crop production while optimizing the workforce and minimizing maintenance costs [5, 6]. However, there are several hurdles to an efficient implementation of WUSNs for sustainable smart agriculture. They are mainly related to the communication range and the energy consumption of the USs [7]. For instance, due to the highly attenuating communication channels, much more energy is required by USs in WUSNs than terrestrial wireless sensor networks (WSNs) to ensure reliable data transmissions through soils [8]. Furthermore, a long WUSN life must be achieved in sustainable smart agriculture as it is impractical to periodically replace USs' battery. To meet these demands and improve the network throughput, the radio frequency (RF) energy harvesting (EH) technique has been recently proposed for various sustainable underground applications, leading to a new concept: wireless-powered underground sensor networks (WPUSNs) [4, 9–11].

In a typical WPUSN, the USs harvest energy from a dedicated power source (PS), where the wireless energy transfer (WET) technique can be readily applied [12]. Then, they use the harvested energy for delivering the sensed data to an access point (AP) through wireless information transmission (WIT). This process was originally defined as the harvest-then-transmit (HTT) protocol, which has rapidly gained interest in the WSNs community, e.g., [13, 14]. Note that compared with terrestrial wireless-powered communication networks (WPCNs), HTT-based WPUSNs require a much longer time for harvesting energy before a reliable WIT can be achieved due to the high attenuation introduced by soils. Thus, urgent information transmission cannot be easily established in WPUSNs, especially when the USs are far away from the AP. To overcome this challenge, common solutions may include increasing the transmit power of

ORCID(s):

the PS and/or adopting multiple antennas technologies [11]. However, these approaches are often bulky, pricey, and potentially inefficient for WPUSNs.

On the other hand, the backscatter communication (BSC) technique [15], which allows the devices to communicate wirelessly without active RF transmissions, may be more appealing. Specifically, the sensors transmit data via reflecting and modulating the incident RF signals by adapting the level of antenna impedance mismatch to vary the reflection coefficient [16, 17]. As no active RF signal generation is required, the BSC technique can be incorporated in WPCNs to improve the overall network throughput. Furthermore, compared with the two-phase HTT protocol, the BSC technique can effectively reduce communication latency, thus can support urgent data transmission.

Backscatter-assisted WPCNs (BS-WPCNs) have been proposed and evaluated in several terrestrial scenarios. For instance, the user-specific time allocation that maximizes the total network throughput in a multi-user BS-WPCN was proposed in [18]. Meanwhile, the time and transmit beamforming that maximizes the throughput of BS-WPCNs was evaluated in [19] by considering the homogeneous and heterogeneous network scenarios. The authors in [20] formulated a time and power optimization problem in a multi-carrier BS-WPCN, where a maximum transmit power constraint at the PS and a minimum circuit power consumption constraint at the devices were considered. To improve the transmission rate of BSC, the study in [21] developed an optimal time scheduling scheme based on the compressive spectrum sensing technique to detect ambient RF signals for performing EH or BSC.

Despite extensive efforts on the resource allocation optimization, most of the existing works ignore the two key factors for BS-WPCNs. The first is the EH model. Observe that the above studies only consider a simple linear EH model, implying the received RF power at the device is directly proportional to the input power level. The measurements in [22, 23] evince that the EH process is, however, non-linear in practice, as described in Section 3.2.1. As a consequence, the mechanisms that are designed based on the conventional linear EH model would lead to resource mismatch and performance deterioration in practical BS-WPCNs. Therefore, realistic EH models are compulsory to evaluate the performance of multi-user BS-WPCNs. The second key factor is the influence of underground soils. The underground path losses are severely influenced by complex underground soil conditions. For instance, underground channel conditions change with precipitation-enforced soil moisture throughout the year [7, 8]. Therefore, it remains unclear whether the introduction of BSC technique to WPUSNs would improve the network throughput.

Our current study is oriented to tackle the above challenges. To the best knowledge of the authors, this study is the first one to investigate the feasibility and effectiveness of BSC technology in WPUSNs. Its main contributions are summarized as follows:

1. Considering implementation issues, we conceptualize a backscatter-assisted WPUSN (BS-WPUSN) by defining a sophisticated system model, in which all the USs can not only harvest RF energy from the above-ground PS, but also backscatter the RF signals to the AP.
2. We formulate an optimization problem to maximize the overall network throughput by properly scheduling the time required by each US for BSC, WET, and WIT processes. Each US is subject to quality of service (QoS) constraints specified by a demodulated signal-to-noise ratio (SNR) threshold at the AP. The optimization problem considers the saturation non-linear EH model [23] which can accurately capture the characteristics of practical EH circuits. We prove that the resulting problem is convex and exploit the interior-point method to find its optimal solution.
3. Through simulations of real-world agriculture scenarios, we demonstrate that our proposed model can significantly improve the network throughput compared to two baseline solutions: Underground HTT (U-HTT) [9] and Underground-BSC (U-BSC) [16].
4. The numerical results reveal that the network and underground factors strongly affect the time allocation and network throughput. In some high-attenuation situations, the proposed scheme is switched to the HTT-only mode owing to the failure of the QoS assurance in the BSC mode. These findings provide a guideline for future practical design of sustainable smart agriculture.

The remaining part of the paper is organized as follows. Section 2 describes the structure of a BS-WPUSN and the relevant channel models. Then, Section 3 presents the achievable throughput for the BSC and HTT modes, respectively. In Section 4, we formulate an optimization problem to maximize the overall network throughput with per-user QoS assurances, and discuss implementation issues. Finally, we analyze *in-situ* simulation results in Section 5, and conclude the paper in Section 6. Table 1 lists and defines the acronyms used throughout the article.

Table 1
List of Acronyms

Acronym	Definition
AP	access point
BSC	backscatter communication
BS-WPCN	backscatter-assisted wireless-powered communication network
BS-WPUSN	backscatter-assisted wireless-powered underground sensor network
CDC	complex dielectric constant
EH	energy harvesting
HTT	harvest-then-transmit
MBSDM	mineralogy-based soil dielectric model
PS	power source
QoS	quality of service
RF	radio frequency
SNR	signal-to-noise ratio
TDMA	time division multiple access
UAV	unmanned aerial vehicle
U-BSC	underground backscatter communication
U-HTT	underground harvest-then-transmit
US	underground sensor
VWC	volumetric water content
WET	wireless energy transfer
WIT	wireless information transmission
WPCN	wireless-powered communication network
WPUSN	wireless-powered underground sensor network
WSN	wireless sensor network
WUSN	wireless underground sensor network

2. System Model

2.1. BS-WPUSNs Structure

We consider a multi-user BS-WPUSNs system for sustainable smart agriculture, which consists of a PS, N energy-constrained USs, and an AP, as shown in Fig. 1(a). Let l_{P2U} and d_{P2U} denote the air and underground soil propagation distances from the PS to the USs in the downlink, respectively. Similarly, l_{U2A} and d_{U2A} represent the air and underground soil propagation distances from the USs and the AP in the uplink, respectively. Each US, denoted by U_n, with $n = 1, \cdots, N$, has an EH module and a backscatter circuit, which leverages the RF signals from the PS for backscattering information, so that it can adaptively switch between the HTT and the BSC mode, and correspondingly transmit or backscatter the sensed data to the AP. Notably, the USs cannot work in both HTT and BSC modes simultaneously [24]. When the HTT mode is adopted, U_n harvests energy from the RF signals emitted by the PS, which is subsequently used for WIT. In contrast, when the BSC mode is activated, U_n utilizes the received RF signals to transmit the sensed data to the AP via BSC. Herein, we assume that the AP is capable of detecting and decoding the packet from the modulated BSC signal or triggered by the HTT mode.

A protocol based on time division multiple access (TDMA) is adopted, implying the sequential USs' operation, to avoid the interference among USs. The transmission block T is split into WET/BSC and WIT phases as illustrated in Fig. 1(b). It should be noted that the duration for each transmission block is normalized, i.e., $T = 1$ s, and both phases are divided into N time slots. In the n^{th} time slot of the WET/BSC phase (of duration λ_n), the USs can either backscatter RF signals to transmit sensed data or harvest energy before performing WIT (with duration τ_n). Note that if several USs backscatter at the same time, they will cause a potentially uncontrollable backscattering interference among themselves. Hence, we propose that in WET/BSC period t_0, U_n backscatters signals during its allocated time duration λ_n, whereas all other USs stay silent and harvest energy from the PS. Thus, the total time for WET to U_n during the WET/BSC phase is $t_0 - \lambda_n$. During the WIT period $T - t_0$, the USs use the harvested energy for the active data transmission. Therefore, $\boldsymbol{\lambda} = [\lambda_1 \cdots \lambda_N]^{\mathrm{T}}$ and $\boldsymbol{\tau} = [\tau_1 \cdots \tau_N]^{\mathrm{T}}$ denote respectively the vectors of BSC and WIT time in the system, as described in Fig. 1(b). To improve the network throughput, we should carefully formulate the time allocation of both BSC and HTT modes for each node based on the channel state information. Note that the energy consumption generated by the requesting and receiving processes of the USs is ignored in this study.

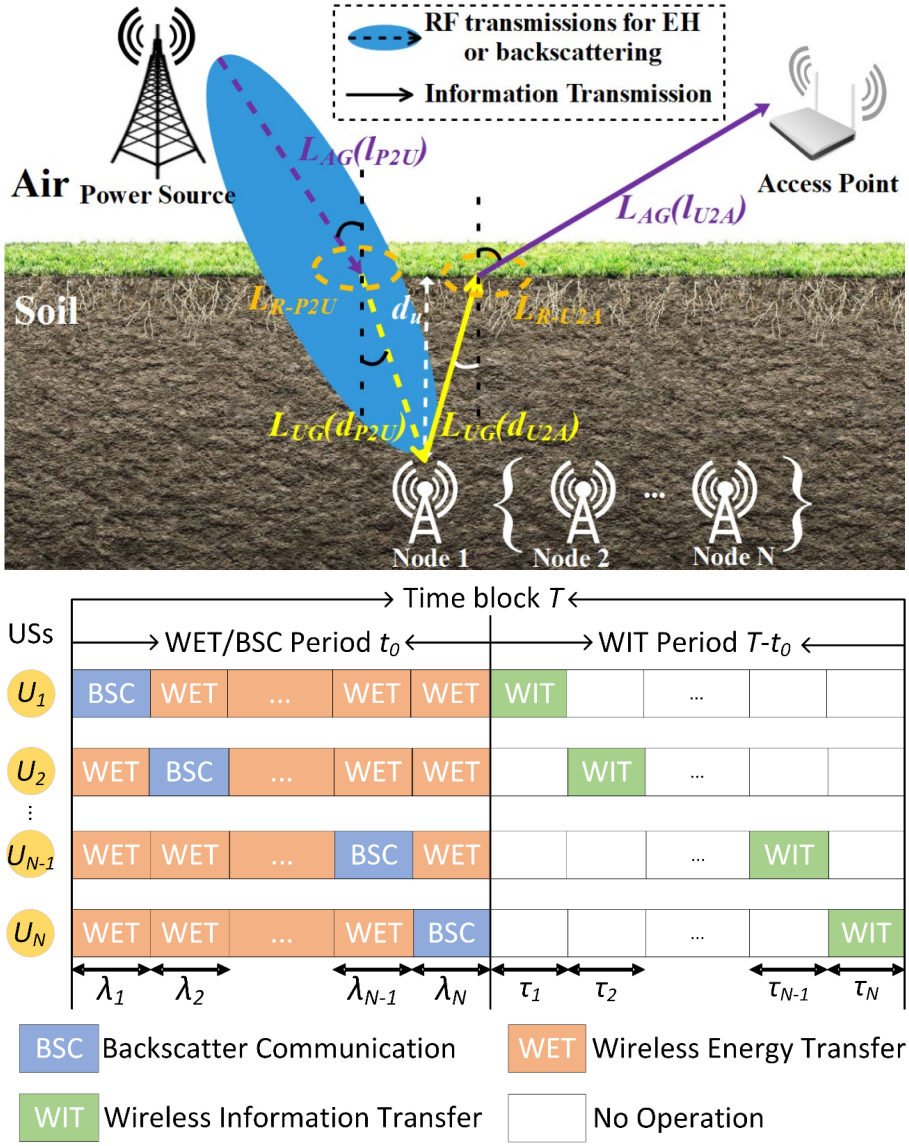

Figure 1: A multi-user BS-WPUSNs system. (a) System model (top). (b) Time block (bottom).

2.2. Channel Model

We model the channels established between the PS and the sensors in the downlink, and between the sensors and the AP in the uplink. Herein, we adopt the modified Friis-based model developed in [25, 26] to quantify the path losses in the downlink and uplink. This channel model considers the refraction loss in the air-ground interface and utilizes the mineralogy-based soil dielectric model (MBSDM), which facilitates an accurate prediction of the complex dielectric constant (CDC) of soil [27]. In [25, 26], the channel model is validated by *in-situ* experiments, which revealed a sufficiently accurate estimate of the attenuation for both links. Therefore, this channel model is applied in Section 2.2.1 and 2.2.2 to accurately quantify the path losses in the proposed BS-WPUSN.

2.2.1. Downlink channels

According to [25, 26], the received signals' average power at U_n can be calculated by the Friis equation as

$$P_{ru}^{n} = \frac{P_P G_P G_U \left|h_d\right|^2}{L_{P2U}^{n}}, \tag{1}$$

$$L_{P2U}^{n} = L_{AG}^{n}(l_{P2U}) L_{R-P2U}^{n} L_{UG}^{n}(d_{P2U}), \tag{2}$$

where P_P is the transmit power of the PS, h_d is the small-scale fading coefficient in the downlink, L^n_{P2U} comprises the power losses in the downlink channel, while G_P and G_U are the antenna gains at the PS and the USs, respectively. In this study, we assume the channel coefficients are perfectly known and/or vary very slowly [28], thus, set $|h_d|^2 = 1$ without loss of generality. Later, in Section 4.2, we discuss implementation issues, including the estimation of the channel coefficients. Moreover, the power losses come from three sources: the above-ground air attenuation, L_{AG}, the refraction loss at the air-soil interface, L_{R-P2U}, and the underground soil attenuation, L_{UG}, as depicted in Fig. 1(a). Mathematically, they are modeled as

$$L^n_{AG}(l_{P2U}) = \left(\frac{4\pi f l_{P2U}}{c}\right)^2, \tag{3}$$

$$L^n_{R\_P2U} = \left(\frac{\sqrt{\left(\sqrt{\varepsilon'^2 + \varepsilon''^2} + \varepsilon'\right)/2} + 1}{4}\right)^2, \tag{4}$$

$$L^n_{UG}(d_{P2U}) = \left(\frac{2\beta d_{P2U}}{\exp(-\alpha d_{P2U})}\right)^2, \tag{5}$$

where f is the operation frequency and c represents the speed of light in air. In addition, α and β are the attenuation constant and phase shifting constant, respectively, which are given by

$$\alpha = 2\pi f \sqrt{\frac{\mu_r \mu_0 \varepsilon' \varepsilon_0}{2}\left[\sqrt{1 + \left(\frac{\varepsilon''}{\varepsilon'}\right)^2} - 1\right]}, \tag{6}$$

$$\beta = 2\pi f \sqrt{\frac{\mu_r \mu_0 \varepsilon' \varepsilon_0}{2}\left[\sqrt{1 + \left(\frac{\varepsilon''}{\varepsilon'}\right)^2} + 1\right]}. \tag{7}$$

Here, μ_r is the soil's relative permeability, μ_0 is the free-space permeability, ε_0 is the free space permittivity, and ε' and ε'' are the real and imaginary parts of the soil's CDC, respectively, i.e., $\varepsilon = \varepsilon' + j\varepsilon''$. The CDC can be calculated by the MBSDM. Compared with the traditional Peplinski model [29], the MBSDM can provide a more accurate CDC prediction because it is derived from a larger number of soil samples and considers the presence of free and bound water in the soil. Furthermore, the MBSDM requires only three input parameters, i.e., the percentage of clay in soils, the volumetric water content (VWC), and the operating frequency of the electromagnetic signals. The detailed description of MBSDM can be found in [27].

2.2.2. Uplink channels

The total path losses in the uplink as described in Fig. 1(a), L^n_{U2A}, includes three parts: the underground path loss, L_{UG}, the refraction loss from soil to air, L_{R-U2A} and the above-ground path loss, L_{AG}. Hence, the average power of the received signal at the AP is given by

$$P^n_{ra} = \frac{P_U G_U G_A \left|h_u\right|^2}{L^n_{U2A}}, \tag{8}$$

$$L^n_{U2A} = L^n_{UG}(d_{U2A}) L^n_{R-U2A} L^n_{AG}(l_{U2A}), \tag{9}$$

where P_U is the transmit power of U_n, G_A is the antenna gain at the AP, and h_u is the small-scale fading coefficient in the uplink. Similar to the downlink, h_u is assumed normalized in power, i.e., $|h_u|^2 = 1$. Moreover, l_{U2A} denotes the air path length from the USs to the AP, while d_{U2A} is the underground propagation path distance from the USs to the AP. Notably, when the normal incidence of electromagnetic waves propagates from a high-density medium (soil) to a lower density one (air), most of the energy is refracted. Therefore, we assume that L_{R-U2A} can be neglected in this study. Note that (3) and (5) are used to calculate $L^n_{UG}(d_{U2A})$ and $L^n_{AG}(l_{U2A})$.

3. Network Throughput for BSC and HTT Modes

The performance of both, the BSC and HTT modes, influences the total network throughput. Therefore, we analyze the throughput contributions of both modes as follows.

3.1. BSC Mode

During the λ_n amount of time assigned to U_n in the BSC mode, U_n backscatters a fraction η_n of the received power to transmit sensed data to the AP in the uplink. Hence, the tranmit power of U_n, P_U, in the BSC mode is

$$P_U = \eta_n P_{ru}^n = \frac{\eta_n P_P G_P G_U |h_d|^2}{L_{P2U}^n}. \tag{10}$$

Then, the SNR at the AP when U_n backscatters the RF signals, SNR_{A-BSC}, is given by

$$\mathrm{SNR}_{A-BSC}^n = \frac{P_{ra}^n}{\sigma_A^2} = \frac{\eta_n P_P G_P G_U^2 G_A |h_d|^2 |h_u|^2}{L_{P2U}^n L_{U2A}^n \sigma_A^2}, \tag{11}$$

where σ_A^2 is the noise power at the AP, and the last step in (11) comes from leveraging (8) and (10). Finally, the achievable throughput of U_n in the BSC phase is given by

$$\begin{aligned} R_B^n(bps) &= \lambda_n W \log_2\left(1 + \mathrm{SNR}_{A-BSC}^n\right) \\ &= \lambda_n W \log_2\left(1 + \frac{\eta_n P_P G_P G_U^2 G_A |h_d|^2 |h_u|^2}{L_{P2U}^n L_{U2A}^n \sigma_A^2}\right), \end{aligned} \tag{12}$$

where W is the channel bandwidth.

3.2. HTT Mode

3.2.1. Saturation Non-linear EH Model

In previous studies, the energy harvested by U_n in the HTT mode is typically modelled as directly proportional to the received RF power, i.e., linear EH model [18, 21]. However, the conventional linear EH model is only suitable for the case that the received power at the devices is constant. Other than that, it shall be discouraged, especially for a realistic design of resource allocation algorithms. For real-world underground monitoring applications, we adopt the practical saturation non-linear EH model proposed in [23] to characterize the efficiency of the WET at U_n at different input power levels. Recent studies have proven that this saturation non-linear EH model can accurately capture the behavior of practical EH circuits [23, 30].

The energy harvested by U_n in the HTT mode is

$$E_{ru}^n = \frac{M_n\left(\frac{1+\exp(A_n B_n)}{1+\exp\left(-A_n\left(P_{ru}^n - B_n\right)\right)} - 1\right)}{\exp\left(A_n B_n\right)}\left(t_0 - \lambda_n\right), \tag{13}$$

where M_n denotes the maximum harvested power at U_n, i.e., the harvested power at saturation. Constants A_n and B_n are correlated with several circuit specifications, such as resistance, capacitance, and circuit sensitivity, while $\left(t_0 - \lambda_n\right)$ is the total EH time of each U_n. In practice, the parameters of M_n, A_n and B_n can be easily obtained by standard curve fitting because the EH circuit for each U_n is normally fixed.

3.2.2. Achievable Throughput

In the WIT phase, U_n consumes all the harvested energy to transmit the sensed data to the AP. Herein, the tranmit power of U_n, P_U, in the HTT mode is

$$P_U = \frac{\varphi_n E_{ru}^n}{\tau_n}, \tag{14}$$

where φ_n represents the portion of received energy used for WIT. Note that the remaining $(1-\varphi_n)$ portion of the harvested energy supports the circuit operations. Then, the SNR at the AP when U_n transmits its sensed data, SNR^n_{A-HTT}, is expressed as

$$\mathrm{SNR}^n_{A-HTT} = \frac{P^n_{ra}}{\sigma^2_A} = \frac{\varphi_n E^n_{ru} G_U G_A |h_u|^2}{L^n_{U2A}\sigma^2_A \tau_n}, \tag{15}$$

which comes from leveraging (8) and (14). Observe that (15) can be written as $\mathrm{SNR}^n_{A-HTT} = k_n(t_0-\lambda_n)/\tau_n$, where

$$k_n = \frac{M_n \varphi_n G_U G_A |h_u|^2 \left(\frac{1+\exp(A_n B_n)}{1+\exp\left(-A_n\left(\frac{P_P G_P G_U |h_d|^2}{L^n_{P2U}} - B_n\right)\right)} - 1 \right)}{L^n_{U2A}\sigma^2_A \exp\left(A_n B_n\right)}. \tag{16}$$

Finally, the achievable throughput of U_n in the WIT phase can be calculated as

$$\begin{aligned} R^n_H(bps) &= \tau_n W \log_2\left(1+\mathrm{SNR}^n_{A-HTT}\right) \\ &= \tau_n W \log_2\left(1+\frac{k_n(t_0-\lambda_n)}{\tau_n}\right). \end{aligned} \tag{17}$$

4. QoS-Aware Sum-Throughout Maximization

In this study, we aim to improve the network throughput of both BSC and HTT modes. This implies more sensor data can be successfully transmitted to the AP under the same power supply, thus, promoting sustainable smart agriculture. An inappropriate time duration allocated for BSC, WET, and WIT will worsen the network reliability and lower the network throughput. Therefore, we manage to find the optimal time allocation (i.e., the optimal time allocation vectors $\boldsymbol{\lambda}$ and $\boldsymbol{\tau}$ as illustrated in Fig. 1(b)) to maximize the network throughput by considering the time constraints and the QoS requirements.

4.1. Problem Formulation and Solution

In the BSC mode, a backscattered signal is assumed to be correctly demodulated/detected at the AP when $\mathrm{SNR}^n_{A-BSC} \geq \gamma,\ n=1,\cdots,N$, where γ represents an SNR threshold. If this premise is not satisfied, we propose switching to the HTT-only mode. Based on this condition, the QoS-aware sum-throughput maximization problem in the BS-WPUSN with multiple USs is formulated as

$$(\mathrm{P1}):\ \max_{\{\lambda_n\},\{\tau_n\}} R_{sum} = \sum_{n=1}^{N}\left(R^n_B + R^n_H\right) \tag{18a}$$

$$s.t.\ t_0 + \sum_{n=1}^{N}\tau_n \leq 1, \tag{18b}$$

$$\sum_{n=1}^{N}\lambda_n = t_0, \tag{18c}$$

$$0 \leq t_0 \leq 1, \tag{18d}$$

$$0 \leq \lambda_n \leq t_0,\ n=1,\cdots,N, \tag{18e}$$

$$0 \leq \tau_n \leq 1-t_0,\ n=1,\cdots,N, \tag{18f}$$

$$\mathrm{SNR}^n_{A-HTT} \geq \gamma,\ n=1,\cdots,N, \tag{18g}$$

where $\sum_{n=1}^{N} R^n_B$ is the throughput produced from the BSC mode, which is determined by the time allocation vector $\boldsymbol{\lambda}$, while $\sum_{n=1}^{N} R^n_H$ is the throughput of the HTT mode, which is a function of the time allocation vectors $\boldsymbol{\lambda}$ and $\boldsymbol{\tau}$. Furthermore, $\mathrm{SNR}^n_{A-HTT} = k_n(t_0-\lambda_n)/\tau_n$, (18b)-(18f) correspond to the time constraints and (18g) is the QoS assurance in the HTT mode.

We firstly prove that (P1) is a convex optimization problem. Note that R_H^n is the perspective function of $f(t_0, \lambda_n) = \log_2(1+k_n(t_0-\lambda_n))$. As the perspective operation preserves concavity, the concavity of R_H^n can be proved by validating that $f(t_0, \lambda_n)$ is a jointly concave function of t_0 and λ_n. For this, we find the Hessian matrix of the objective function, which is given by

$$\mathbf{H}_n = \begin{bmatrix} -1 & 1 \\ 1 & -1 \end{bmatrix} \frac{k_n^2}{\left(1 + k_n\left(t_0 - \lambda_n\right)\right)^2 \ln 2}. \tag{19}$$

Now, given an arbitrary real vector $\mathbf{v} = [v_1, v_2]^{\mathbf{T}}$, we have

$$\mathbf{v}^{\mathbf{T}}\mathbf{H}_{\mathbf{n}}\mathbf{v} = -\frac{k_n^2}{\left(1 + k_n\left(t_0 - \lambda_n\right)\right)^2 \ln 2}\left(v_1 - v_2\right)^2 \leq 0. \tag{20}$$

Then, since R_B^n is a linear function of λ_n, we can conclude that the objective function R_{sum} in (18a) is concave as it is the sum of two concave functions. Meanwhile, (18b)-(18f) are all affine and (18g) is equivalent to $k_n(t_0 - \lambda_n) \geq \tau_n\gamma,\ n \in \{1, \cdots, N\}$ which is linear. Therefore, (P1) is a convex optimization problem, which can be effectively addressed by adopting the interior-point method [31]. Consequently, we can utilize optimization tools (e.g., CVX [32] and *fmincon* function from MATLAB [33]) to solve it. In general, parallel processing/simulation is recommended to speed up the solution, especially in large-scale setups. In addition, the overall computational complexity of the interior-point method in this work is $\mathcal{O}\left(\frac{\sqrt{N}}{\epsilon}\right)$, where ϵ represents the iterative accuracy.

4.2. Implementation of the Proposed Strategy

In practice, the proposed time allocation for the considered BC-WPUSNs can be implemented as illustrated in Fig. 2. The system diagram is divided into three segments: (1) ID assignment; (2) time allocation; and (3) BSC/HTT process.

1. ID assignment: Each US sends a service request to the PS. The PS replies with the assigned US's ID.
2. Time allocation: The PS sequentially transmits the pilots to the corresponding ID-assigned USs, which immediately backscatter them to the AP. The AP estimates each composite downlink-uplink channel by the received pilots before summarizing and forwarding the information of all channels to the PS. The signal propagation processes of downlink and uplink are illustrated in Fig. 1(a). The PS applies the interior-point method to solve (P1) based on the received channel state information, which implies computing the optimal time allocation $\boldsymbol{\lambda} = [\lambda_1 \cdots \lambda_N]^{\mathrm{T}}$ and $\boldsymbol{\tau} = [\tau_1 \cdots \tau_N]^{\mathrm{T}}$ with the time constraints and the QoS assurance. After that, the PS broadcasts the allocation results to the USs. Note that the determination of time allocation is conducted at the PS. Thus, the USs can save energy and further extend their operation lifetime.
3. BSC/HTT process: Once all USs have received the allocated time duration of BSC, WET and WIT, time synchronization [34] is executed in the whole system, and then each U_n sends a request to the PS for triggering the BSC/HTT process. Upon receiving the request, the PS starts broadcasting the RF signal. As depicted in Fig. 1(b), under the allocated WET/BSC period t_0, the U_n backscatters the sensed data to the AP during λ_n and harvests the energy from the PS in the period of $t_0 - \lambda_n$. Eventually, all USs use energy harvested from the PS in the downlink to transmit their sensed data to the AP in the uplink via a TDMA scheme.

5. Performance Elevation and Discussion

5.1. Experimental Setup and Configurations

To evaluate the performance of BS-WPUSNs, we choose a realistic center-pivot irrigation farm as our study scenario, where several USs are equidistantly deployed. To reflect the real performance of our proposed system in such a study case, we used the *in-situ* soil characteristics obtained from [35], e.g., clay content of soils, to obtain the realistic attenuation of PS-to-USs and USs-to-AP, as shown in Fig. 1(a). The system bandwidth is set to 125 kHz and the carrier frequency to 433 MHz, which are suitable for general underground wireless communications. The isotropic antennas are adopted in the system and the antenna gains for the PS, U_n and the AP are all set to 0 dBi. The transmit power of the PS is 30 dBm, while the horizontal distance from the PS to U_n is assumed to be 1 m such that enough

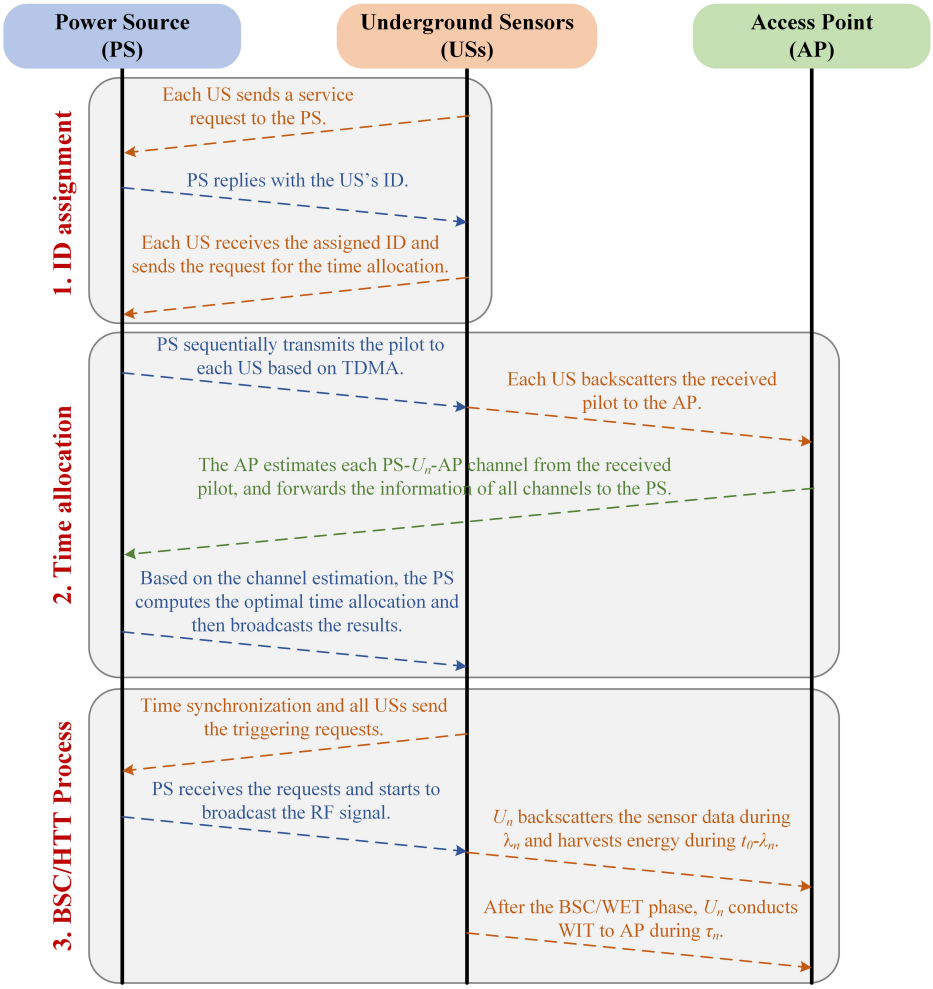

Figure 2: The system diagram of the conceptualized BS-WPUSNs.

power is received at the USs. The AP is 1.5 m above the ground surface to avoid the effects of the lateral wave [25]. The backscatter coefficient and energy conversion efficiency are both set to 0.6 [20]. The noise power and the demodulated SNR threshold at the AP are assumed as -117 dBm and -20 dB, respectively [25]. For the practical EH circuit, we set $M_n = 9.2$ μW which corresponds to the maximum harvested power of U_n [19]. Besides, $A_n = 150$ and $B_n = 0.0014$ are obtained by applying a standard curve fitting algorithm to the measurement data provided in [30]. Unless otherwise specified, the horizontal distance between the USs and the AP is 50 m, the number of USs is 32, the burial depth of U_n is 0.35 m and the VWC of the soils is 0.1. The key simulation parameters are summarized in Table 2.

5.2. Benchmark Schemes

We compare our proposed scheme with two well-established solutions:

- U-HTT [9], where the BSC mode does not exist. Here, the first phase of duration t_0 is completely devoted to WET. Meanwhile, the second phase of duration $T - t_0$ is allocated for WIT from the USs. More specifically, U_n harvests energy from the AP for a duration t_0 and then transmits the sensed data within the period τ_n in the WIT phase.

- U-BSC [16], where the whole time block is divided into equal time slots for performing BSC at each U_n. There is no HTT process in this scheme. Interestingly, the performance of such an approach has not been previously studied in the context of underground wireless network.

It should be noted that the strategy for implementing U-HTT and U-BSC is identical to that outlined in Section 4.2.

Table 2
Simulation Parameters and Configurations

Parameters	Values
hline Carrier center frequency (f)	433 MHz
Bandwidth (W)	125 kHz
Antenna gains (G_P, G_U, G_A)	0 dBi
Transmit power of the PS (P_P)	30 dBm
Horizontal distance in the downlink (H_{P2U})	1 m
Horizontal distance in the uplink (H_{U2A})	*var* (50 m by default)
AP height (H)	1.5 m
Backscatter coefficient (η_n)	0.6
Energy conversion efficiency (φ_n)	0.6
Noise power at the AP (σ_n)	-117 dBm
Demodulated SNR threshold at the AP (γ)	-20 dB
Number of USs (N)	*var* (32 by default)
Burial depth (d_u)	*var* (0.35 m by default)
VWC	*var* (0.1 by default)
Clay (C)	38% [35]
Harvested power at saturation (M_n)	9.2 μW [19]
Fitting parameters of the EH model (A_n, B_n)	150, 0.0014 [30]

5.3. Numerical Results and Analysis

5.3.1. Performance Impact of Network Parameters

Herein, we study the impact of two key network parameters, i.e., communication distance and the number of nodes, on the network throughput and the time allocation for U-HTT, U-BSC and our proposed solution. In a practical smart agriculture scenario, the USs need to be deployed in different vertical and horizontal positions to collect the local soil's information, implying the various communication distances between the USs and the AP. On the other hand, the deployment scope in agricultural fields and crop type also determines the number of USs should be deployed [1]. To orient for different smart farming applications, it is necessary to investigate the effects of these two key network parameters (i.e., communication range and US's number) on the performance of our proposed BS-WPUSNs.

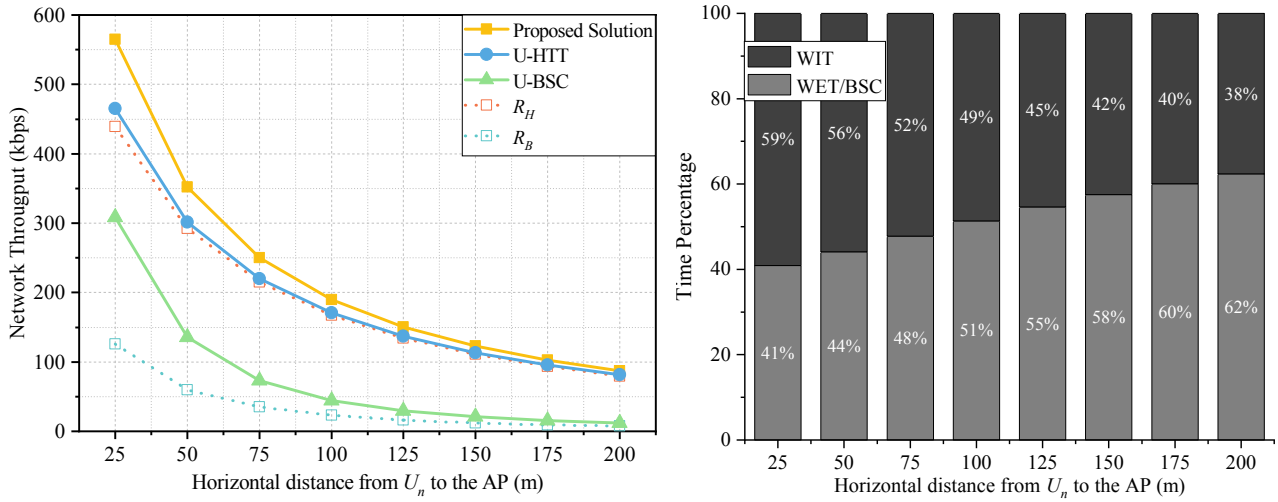

Figure 3: (a) The network throughput (left), and (b) the time allocation (right) of the proposed solution compared to two benchmark schemes with various US-to-AP horizontal distances.

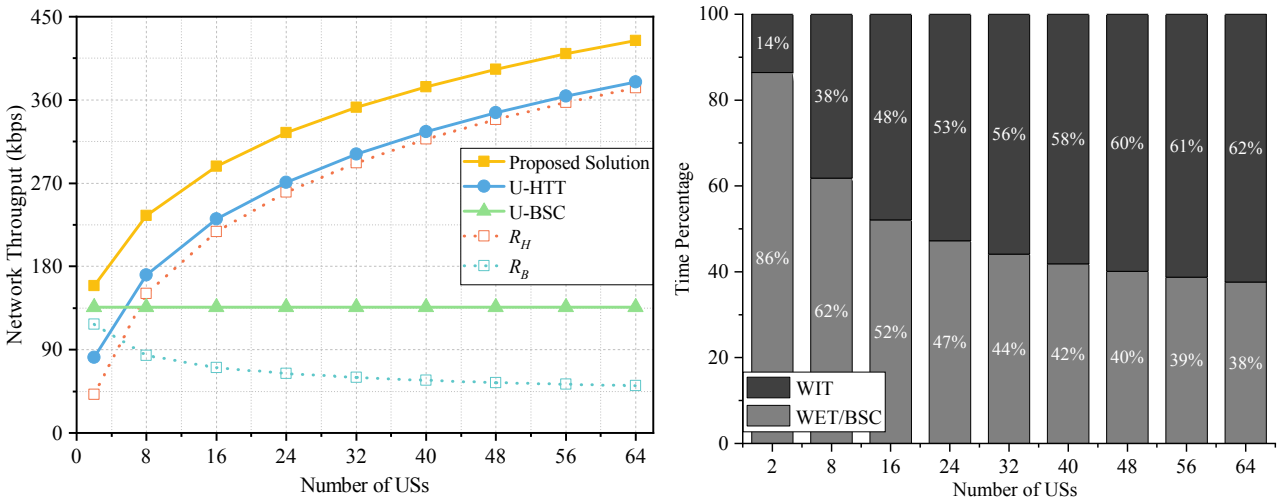

Figure 4: (a) The network throughput (left), and (b) the time allocation (right) of the proposed solution compared to two benchmark schemes with varying the number of USs.

Table 3
Solution Runtime of (P1) under Different Number of USs

Node number	2	4	8	16	32	64	128
Runtime (s)	0.7	0.8	1.1	2.1	5.5	15.5	63.1

Fig. 3(a) depicts the network throughput as a function of the distance from the USs to the AP. Since the power received by the AP decreases when the propagation range increases, the total network throughput decreases from 564.79 kbps at 25 m to 87.32 kpbs at 200 m. It can be observed that the throughput earnings of our proposed solution over U-HTT reduces when the distance between the USs and the AP increases. For instance, the network throughput gain is reduced from 21.35% at 25 m to 7.30% at 200 m. Meanwhile, the network throughput gain by our proposed solution is increased from 83.32% at 25 m to 616.26% at 200 m, compared with U-BSC. Herein, the different performance of these two benchmarks stems from the fact that U-HTT sustains a high network throughput, which can be compensated by assigning more time to WET with the large US-to-AP distance, while the throughput of the BSC scheme is solely affected by the communication distance. Overall, the available network throughput of our proposed solution can surpass 350 kbps at $H_{U2A} = 50$ m, which is better than U-HTT and U-BSC. In addition, Fig. 3(b) displays the time allocation of the proposed solution for $N = 32$, $C = 38\%$ and VWC $= 0.1$. Note that as H_{U2A} increases, the time duration allocated for the WET/BSC phase increases to ensure the reliable BSC and WIT, i.e., satisfying the required QoS at the AP.

Fig. 4(a) exhibits the network throughput as a function of the number of USs. First of all, we provide the solution runtime of (P1) by different number of USs as summarized in Table 3, where the optimization is conducted in a Matlab R2021b on a Windows 10 platform with Intel Core i7-6820HK 2.7 GHz CPU and 16 GB RAM. As the number of sensors increases (i.e., the more variables), the runtime increases from 0.7 s to 63.1 s. This computational delay is acceptable in smart agriculture applications because the underground environment is relatively static, and the VWC of soils does not vary drastically with time [36]. When more USs are deployed, the overall network throughput for our proposed solution and U-HTT gets higher, while the overall network throughput of U-BSC remains 135.89 kbps independently upon the number of nodes. Moreover, since multiple USs can harvest energy simultaneously while they cannot backscatter information at the same time, our proposed solution tends to allocate more time to the HTT mode rather than to the BSC mode, as the number of USs increases as shown in Fig. 4(b). In addition, thanks to the high received power at the USs under this underground parameter configuration and the more time allocated for each US, U-BSC can provide higher network throughput than U-HTT as the number of USs is less than 4. Noteworthy, in all cases, our proposed solution outperforms the other schemes in terms of the overall network throughput.

5.3.2. Performance Impact of Underground Parameters

Herein, we explore the influence of two key underground factors, i.e., burial depth and VWC of the soils, on the network throughput for U-HTT, U-BSC, and our proposed solution. Dealing with smart agriculture applications, one needs to consider the fact that the roots of different crops reach different depths [37]. Therefore, the sensors shall be buried at various depths to monitor soil conditions such as moisture and salinity efficiently. Hence, it is of great significance to evaluate the performance of our proposed solution under various burial depths. Similarly, due to the VWC of soils varying with precipitation or irrigation, we need to investigate the robustness of the proposed system under various VWCs.

Fig. 5(a) shows the network throughput decreases as the burial depth increases. Burial depth affects not only the power of the backscattered signal at the USs, but also the received signal quality at the AP. For instance, the overall network throughput of our proposed solution reduces from 1355.00 kbps at $d_u = 0.1$ m to 5.64 kbps at $d_u = 0.8$ m. On the other hand, the performance of our proposed solution is noticeably superior to the two other baseline schemes when the burial depth is shallower than 0.7 m. For example, at the burial depth of 0.35 m (which is suitable for potatoes and carrots), the proposed solution can realize an average of 12 % and 358% increase in throughput compared to U-HTT and U-BSC, respectively. Since the QoS assurance cannot be satisfied in the BSC mode at $d_u \geq 0.7$ m, the network throughput of U-BSC drops to 0, and at the same time, the proposed solution is automatically switched to the HTT-only mode. Notably, the network throughput of the HTT mode in our proposed solution, i.e., R_H, increases as the burial depth increases in the range $d_u \leq 0.15$ m. This observation is explained by the higher throughput gains achieved from the BSC mode compared to the HTT mode at such shallow depths. It can be further validated by the results of U-BSC and U-HTT in the range $d_u \leq 0.15$ m. Fig. 5(b) shows the results of the time allocation at various burial depths. One can see that the time duration allocated for the WET/BSC phase decreases within a depth of 0.25 m and then increases with depths ranging from 0.25 m to 0.8 m. More specifically, our proposed solution firstly takes more time on the BSC mode to enhance the overall network throughput at the depth of 0.1 m; then, the time duration allocated for the WET/BSC phase decreases when the burial depth varies from 0.15 m to 0.25 m because the throughput gain achieved by the BSC mode significantly reduces. Finally, the USs need more time to ensure the QoS in the BSC mode and harvest more energy for a reliable WIT at deeper burial depths ($d_u \geq 0.25$ m), thus the time duration assigned for the WET/BSC phase starts to increase gradually.

Fig. 6(a) displays the network throughput with the soils' VWC ranging from 0.05 to 0.3. It reveals that our proposed solution provides a higher overall network throughput than the two other baseline schemes within the range of VWC ≤ 0.2. For instance, at VWC $= 0.1$, the network throughput of our proposed solution is increased by 16.83% and 159.02% compared with U-HTT and U-BSC, respectively. However, the superiority of our proposed solution over U-HTT is strongly affected by the VWC of the soils, especially under high VWC conditions. For instance, the network

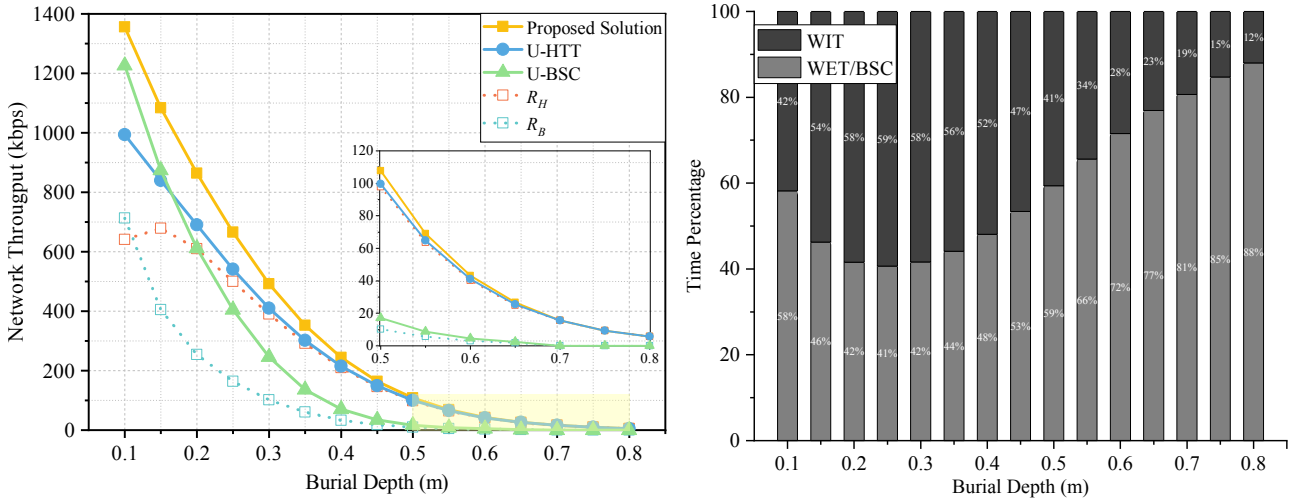

Figure 5: (a) The network throughput (left), and (b) the time allocation (right) of the proposed solution compared to two benchmark schemes at different burial depths of USs.

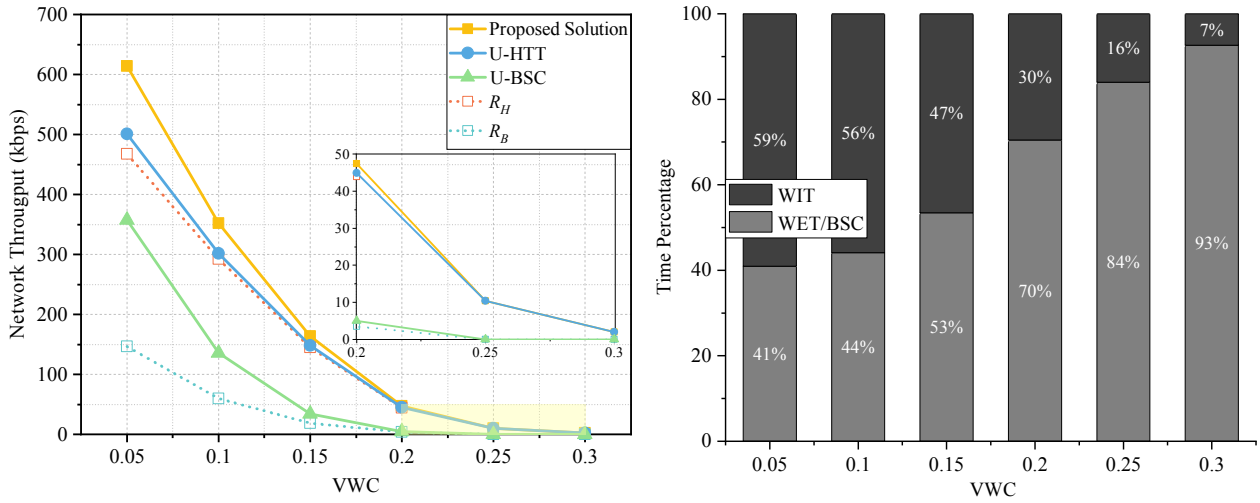

Figure 6: (a) The network throughput (left), and (b) the time allocation (right) of the proposed solution compared to two benchmark schemes with varying VWC of the soils.

throughput gain is reduced from 22.54% at VWC = 0.05 to 5.56% at VWC = 0.2, while the proposed solution is switched to the HTT-only mode when the VWC of the soils surpasses 0.2 owing to the unsatisfied QoS requirement in the BSC mode. A higher VWC of the soils significantly increases the underground signal attenuation, which leads to a lower received energy in the BSC/WET phase at the USs. Therefore, much higher transmitted power is required in the BSC mode and HTT mode for the QoS assurance at the AP. Consequently, the time duration allocated for the WET/BSC phase increases with the VWC of the soils, as shown in Fig. 6(b).

6. Conclusion

Motivated by extending the operation lifetime of WUSNs for sustainable smart agriculture, we advocated incorporating BSC technology into WPUSNs to improve the network throughput and energy efficiency. We firstly proposed and characterized a multi-user BS-WPUSN. Then, we formulated the time allocation that maximizes the BS-WPUSN throughput while considering a practical non-linear EH model and QoS requirements. Moreover, we discussed the implementation guidelines for our proposed solution. We performed simulations corresponding to a realistic farming scenario, and our results revealed that the proposed solution can realize an average of 12 % and 358% increase in throughput compared to two state-of-the-art benchmark schemes: U-HTT and U-BSC, respectively, when the sensors are buried at 0.35 m. However, its performance gain is inevitably affected by the network conditions (e.g., the US-to-AP horizontal distance and the number of USs) as well as the harsh underground environments (e.g., the burial depth of US and VWC of soils). More specifically, the throughput gain of the proposed approach decreases with a wider communication range, higher burial depth, and larger VWC. Although more deployed USs can improve the total network throughput, it leads to longer runtime and more energy required to acquire accurate channel state information. Nonetheless, we believe the suggested approach is perspective for the small-scale centre-pivot irrigation farms. Furthermore, our results also revealed the performance interplay between network throughput, time allocation, network configuration and underground parameters. For instance, the more time allocated for the BSC/WET stage ensures the QoS assurance for both the BSC and HTT modes in a case of strong soil attenuation. On the other hand, the time duration allocated for WIT period increases with the number of USs, as the higher throughput gain can be achieved in the HTT mode compared to the BSC mode. We believe that our preliminary study will pave the way for deploying environmentally sustainable smart agriculture and facilitate further studies based on this concept.

7. Future Works

The simulations evinced the feasibility of our BS-WPUSN system in sustainable smart agriculture. Meanwhile, the advocated approach can also be generalized to other sustainable underground scenarios, such as underground pipelines

and smart seismic quality control. However, there are several potential challenges and future research directions for the practical deployment of the BS-WPUSN system, especially in the scenarios of massive USs connectivity, large-scale agricultural fields, and high-VWC underground conditions.

- In smart agriculture applications, the seasonal crop growth cycles should be considered as they will temporarily affect the network connectivity. The field experiments shall be conducted to accurately evaluate the impact of seasonal crops on the network reliability in future works.
- The maximum transmit power is fixed in this study to overcome the high attenuation of underground soils. However, due to the dynamic and strong heterogeneity of underground environment, each US features different path losses and data traffic demands [11], which has been highlighted in the simulation results of different communication distances, burial depths, and VWC. Equipping the PS with multiple-antenna is a promising solution to eliminate the unfair distribution of harvested energy resources and further improve the network throughput. This allows beamforming techniques to allocate the required proportions of the transmit power in diverse directions [38]. Therefore, investigating the effectiveness of joint time and energy allocation for the proposed BS-WPUSN by considering diverse data traffic requirements, i.e., the periodic or Poisson-traffic for data transmission, is a prospective research direction for practical smart agriculture applications.
- To facilitate the proposed system in a large farm, one may consider mounting the PS onto agricultural unmanned aerial vehicles (UAVs) [39], or deploying multiple PSs [40] to cover the whole area. This inspires the study of the effective design of UAV's trajectory planning and time allocation and the efficient deployment of multiple PSs for the proposed BS-WPUSN system.
- Note that we have ignored the energy consumed for signalling purposes throughout our work. However, broadcasting the pilot beacon for perfect channel state estimation becomes exceptionally costly or impractical in BS-WPUSNs, especially when powering numerous USs. Therefore, to avoid high energy expenditure, the uncoordinated WET scheme without channel state information developed in [41, 42] may be a sensible solution in a massive BS-WPUSNs scenario and will constitute our future research direction.

Declaration of competing interest

The authors declare that they have no known competing financial interests or personal relationships that could have appeared to influence the work reported in this paper.

Acknowledgements

This work was supported in part by the National Natural Science Foundation of China under Grants No. 42074179 and No. 42211530077 (joint with The Royal Society International Exchanges 2021 Cost Share: IEC\NSFC\211286), the Academy of Finland, 6G Flagship program under Grant 346208, and the China Scholarship Council.

References

[1] M. C. Vuran, A. Salam, R. Wong, S. Irmak, Internet of underground things in precision agriculture: Architecture and technology aspects, Ad Hoc Networks 81 (2018) 160–173.
[2] K. Lin, T. Hao, Link Quality Analysis of Wireless Sensor Networks for Underground Infrastructure Monitoring: A Non-Backfilled Scenario, IEEE Sensors Journal 21 (2021) 7006–7014.
[3] N. Saeed, M.-S. Alouini, T. Y. Al-Naffouri, Toward the Internet of Underground Things: A Systematic Survey, IEEE Communications Surveys Tutorials 21 (2019) 3443–3466.
[4] G. Liu, Data Collection in MI-Assisted Wireless Powered Underground Sensor Networks: Directions, Recent Advances, and Challenges, IEEE Communications Magazine 59 (2021) 132–138.
[5] I. Charania, X. Li, Smart farming: Agriculture's shift from a labor intensive to technology native industry, Internet of Things 9 (2020) 100142.
[6] O. Debauche, J.-P. Trani, S. Mahmoudi, P. Manneback, J. Bindelle, S. A. Mahmoudi, A. Guttadauria, F. Lebeau, Data management and internet of things : A methodological review in smart farming, Internet of Things 14 (2021) 100378.
[7] K. Lin, T. Hao, Adaptive Selection of Transmission Configuration for LoRa-based Wireless Underground Sensor Networks, in: IEEE Wireless Communications and Networking Conference (WCNC), 2021, pp. 1–6. doi:10.1109/WCNC49053.2021.9417371.
[8] A. Salam, M. C. Vuran, S. Irmak, A Statistical Impulse Response Model Based on Empirical Characterization of Wireless Underground Channels, IEEE Transactions on Wireless Communications 19 (2020) 5966–5981.

[9] G. Liu, Z. Wang, T. Jiang, QoS-Aware Throughput Maximization in Wireless Powered Underground Sensor Networks, IEEE Transactions on Communications 64 (2016) 4776–4789.
[10] K. M. Z. Shams, M. Ali, Wireless Power Transmission to a Buried Sensor in Concrete, IEEE Sensors Journal 7 (2007) 1573–1577.
[11] G. Liu, Z. Sun, T. Jiang, Joint Time and Energy Allocation for QoS-Aware Throughput Maximization in MIMO-Based Wireless Powered Underground Sensor Networks, IEEE Transactions on Communications 67 (2019) 1400–1412.
[12] X. Chen, D. W. K. Ng, W. Yu, E. G. Larsson, N. Al-Dhahir, R. Schober, Massive Access for 5G and Beyond, IEEE Journal on Selected Areas in Communications 39 (2021) 615–637.
[13] H. Ju, R. Zhang, Throughput Maximization in Wireless Powered Communication Networks, IEEE Transactions on Wireless Communications 13 (2014) 418–428.
[14] O. L. Alcaraz López, E. M. G. Fernández, R. D. Souza, H. Alves, Wireless Powered Communications with Finite Battery and Finite Blocklength, IEEE Transactions on Communications 66 (2018) 1803–1816.
[15] N. Van Huynh, D. T. Hoang, X. Lu, D. Niyato, P. Wang, D. I. Kim, Ambient Backscatter Communications: A Contemporary Survey, IEEE Communications Surveys Tutorials 20 (2018) 2889–2922.
[16] V. Liu, A. Parks, V. Talla, S. Gollakota, D. Wetherall, J. R. Smith, Ambient Backscatter: Wireless Communication out of Thin Air, in: Proceedings of the ACM SIGCOMM Conference on SIGCOMM, 2013, p. 39–50.
[17] X. Lu, D. Niyato, H. Jiang, D. I. Kim, Y. Xiao, Z. Han, Ambient backscatter assisted wireless powered communications, IEEE Wireless Communications 25 (2018) 170–177.
[18] N. Van Huynh, D. T. Hoang, D. Niyato, P. Wang, D. I. Kim, Optimal Time Scheduling for Wireless-Powered Backscatter Communication Networks, IEEE Wireless Communications Letters 7 (2018) 820–823.
[19] P. Ramezani, A. Jamalipour, Optimal Resource Allocation in Backscatter Assisted WPCN with Practical Energy Harvesting Model, IEEE Transactions on Vehicular Technology 68 (2019) 12406–12410.
[20] Y. Xu, G. Gui, Optimal Resource Allocation for Wireless Powered Multi-Carrier Backscatter Communication Networks, IEEE Wireless Communications Letters 9 (2020) 1191–1195.
[21] X. Liu, Y. Gao, F. Hu, Optimal Time Scheduling Scheme for Wireless Powered Ambient Backscatter Communications in IoT Networks, IEEE Internet of Things Journal 6 (2019) 2264–2272.
[22] J. Guo, X. Zhu, An improved analytical model for RF-DC conversion efficiency in microwave rectifiers, in: IEEE/MTT-S International Microwave Symposium Digest, 2012, pp. 1–3. doi:10.1109/MWSYM.2012.6259492.
[23] E. Boshkovska, D. W. K. Ng, N. Zlatanov, R. Schober, Practical Non-Linear Energy Harvesting Model and Resource Allocation for SWIPT Systems, IEEE Communications Letters 19 (2015) 2082–2085.
[24] P. Zhang, D. Ganesan, Enabling Bit-by-Bit Backscatter Communication in Severe Energy Harvesting Environments, in: 11th USENIX Symposium on Networked Systems Design and Implementation (NSDI 14), 2014, pp. 345–357.
[25] K. Lin, T. Hao, Experimental Link Quality Analysis for LoRa-Based Wireless Underground Sensor Networks, IEEE Internet of Things Journal 8 (2021) 6565–6577.
[26] D. Wohwe Sambo, A. Forster, B. O. Yenke, I. Sarr, B. Gueye, P. Dayang, Wireless Underground Sensor Networks Path Loss Model for Precision Agriculture (WUSN-PLM), IEEE Sensors J. 20 (2020) 5298–5313.
[27] V. L. Mironov, L. G. Kosolapova, S. V. Fomin, Physically and Mineralogically Based Spectroscopic Dielectric Model for Moist Soils, IEEE Transactions on Geoscience and Remote Sensing 47 (2009) 2059–2070.
[28] P. Viswanath, D. Tse, R. Laroia, Opportunistic Beamforming Using Dumb Antennas, IEEE Transactions on Information Theory 48 (2002) 1277–1294.
[29] N. Peplinski, F. Ulaby, M. Dobson, Dielectric Properties of Soils in the 0.3-1.3-GHz Range, IEEE Transactions on Geoscience and Remote Sensing 33 (1995) 803–807.
[30] E. Boshkovska, D. W. K. Ng, L. Dai, R. Schober, Power-Efficient and Secure WPCNs With Hardware Impairments and Non-Linear EH Circuit, IEEE Transactions on Communications 66 (2018) 2642–2657.
[31] S. Boyd, S. P. Boyd, L. Vandenberghe, Convex optimization, Cambridge university press, 2004.
[32] M. Grant, S. Boyd, CVX: Matlab Software for Disciplined Convex Programming, version 2.1, http://cvxr.com/cvx, 2014.
[33] 9.11.0.1837725 (R2021b), MATLAB, Natick, MA, USA, 2021. URL: https://www.mathworks.com/help/optim/ug/fmincon.html.
[34] D. Mills, Internet Time Synchronization: the Network Time Protocol, IEEE Transactions on Communications 39 (1991) 1482–1493.
[35] X. Dong, M. C. Vuran, S. Irmak, Autonomous precision agriculture through integration of wireless underground sensor networks with center pivot irrigation systems, Ad Hoc Networks 11 (2013) 1975–1987.
[36] S. Wang, B. Fu, G. Gao, Y. Liu, J. Zhou, Responses of soil moisture in different land cover types to rainfall events in a re-vegetation catchment area of the loess plateau, china, CATENA 101 (2013) 122–128.
[37] United States Department of Agriculture, Irrigation Guide, 2005. URL: https://www.nrcs.usda.gov/Internet/FSE_DOCUMENTS/nrcs141p2_017640.pdf.
[38] O. L. A. López, H. Alves, R. D. Souza, S. Montejo-Sánchez, E. M. G. Fernández, M. Latva-Aho, Massive Wireless Energy Transfer: Enabling Sustainable IoT Toward 6G Era, IEEE Internet of Things Journal 8 (2021) 8816–8835.
[39] A. D. Boursianis, M. S. Papadopoulou, P. Diamantoulakis, A. Liopa-Tsakalidi, P. Barouchas, G. Salahas, G. Karagiannidis, S. Wan, S. K. Goudos, Internet of Things (IoT) and Agricultural Unmanned Aerial Vehicles (UAVs) in smart farming: A comprehensive review, Internet of Things 18 (2022) 100187.
[40] O. M. Rosabal, O. L. A. López, H. Alves, S. Montejo-Sánchez, M. Latva-Aho, On the Optimal Deployment of Power Beacons for Massive Wireless Energy Transfer, IEEE Internet of Things Journal 8 (2021) 10531–10542.
[41] O. L. A. López, N. H. Mahmood, H. Alves, M. Latva-aho, CSI-Free vs CSI-Based Multi-Antenna WET for Massive Low-Power Internet of Things, IEEE Transactions on Wireless Communications 20 (2021) 3078–3094.

[42] O. L. A. Lopez, N. H. Mahmood, H. Alves, C. M. Lima, M. Latva-aho, Ultra-Low Latency, Low Energy, and Massiveness in the 6G Era via Efficient CSIT-Limited Scheme, IEEE Communications Magazine 58 (2020) 56–61.